

## Transition Metal Iodates. III. Gel Growth and Characterization of Six Cupric Iodates

K. NASSAU, A. S. COOPER, J. W. SHIEVER AND B. E. PRESCOTT

*Bell Laboratories, Murray Hill, New Jersey 07974*

Received March 21, 1973

The only normal cupric iodates previously known were the anhydride  $\text{Cu}(\text{IO}_3)_2$  and its  $2/3$  hydrate, the mineral bellingerrite. Growth from the gel at room temperature simultaneously produced five crystalline phases: in addition to the two above there were two other anhydride phases and a dihydrate  $\text{Cu}(\text{IO}_3)_2 \cdot 2\text{H}_2\text{O}$ . Some of these phases are probably metastable. At  $60^\circ\text{C}$ , crystals of the basic cupric iodate  $\text{Cu}(\text{OH})\text{IO}_3$ , the mineral salesite, also formed. Details of the growth of single crystals, nucleation, morphology, characterization by differential thermal analysis and thermogravimetric analysis, and optical data of these six copper iodates are presented. Structural, magnetic, and other data are presented in Part IV.

### 1. Introduction

Two previous reports (1, 2) (hereafter referred to as I and II) dealt with the preparation and properties of the  $3d$  transition metal iodates, including those of copper in I. Owing to the strongly oxidizing nature of the iodate radical only cupric iodates can be expected, and precipitation or crystallization from water or boiling nitric acid were found to yield only  $\text{Cu}(\text{IO}_3)_2 \cdot \frac{2}{3}\text{H}_2\text{O}$ , the mineral bellingerrite. We have also noted (3) that this compound has at times been erroneously designated  $\text{Cu}(\text{IO}_3)_2 \cdot \text{H}_2\text{O}$ .

On heating bellingerrite to  $300^\circ\text{C}$  the anhydride  $\text{Cu}(\text{IO}_3)_2$  is formed; some of its properties were also reported in I. Since it could not be obtained in crystalline form, attempts were made to use gel growth to obtain crystals. Not only were these attempts successful, but a total of five distinct copper iodate compounds crystallized simultaneously. In Fig. 1 is outlined the interrelationship of these compounds. Figure 1 is based on the preparation conditions, thermal analysis, optical absorption, and analytical results here presented, as well as on numerous X-ray powder diffraction patterns.

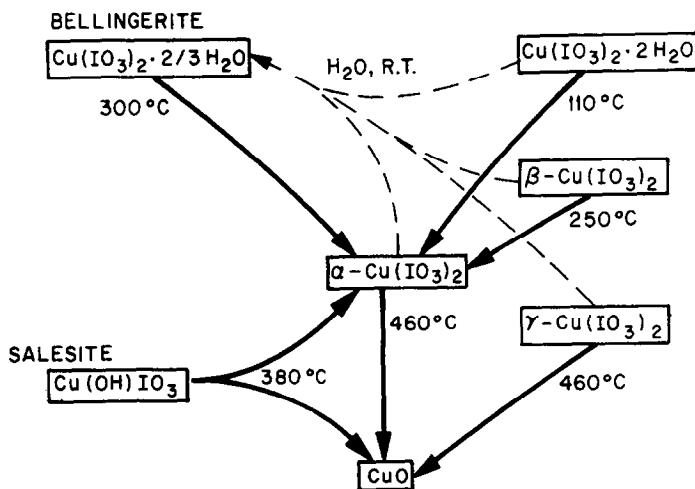


FIG. 1. Transformation relationships among the six copper iodates studied.

The basic iodate  $\text{Cu}(\text{OH})\text{IO}_3$  is known as the mineral salesite. Crystals of this compound were also obtained in gel growth at slightly elevated temperatures, together with some of the other iodates here described, and this compound is also included in Fig. 1.

The following paper (4) contains magnetic, crystallographic, and some nonlinear optic data.

## 2. Experimental Methods

The general technique of gel growth as described by Henisch (5) was followed. Several series of experiments in which concentrations, gel conditions, and temperature were varied were performed in double test tube arrangements (6) designed to duplicate U-tube conditions in a more compact configuration. The tubes held about 10 ml each of gel and the two reagents. When conditions had been optimized a number of runs were also made in large U-tube vessels consisting

of two 125 ml flasks joined by 25 mm o.d. tubing as shown in Fig. 2.

Stock solutions were made from Fischer "Reagent Grade" chemicals as follows: Silicate: sodium meta-silicate ( $\text{Na}_2\text{SiO}_3 \cdot 9\text{H}_2\text{O}$ ) 488 g/liter; copper sulfate (0.3 M):  $\text{CuSO}_4$ , 48 g/liter; iodic acid (0.6 M):  $\text{HIO}_3$  106 g/liter; acetic: glacial acetic acid, 80 ml/liter.

The gels were made by mixing 75 ml of silicate solution with 250 ml acetic solution; 30 ml was poured into each U-tube vessel and permitted to set for 48 hr while open to the atmosphere. Copper sulfate solution (100 ml) was then added to one side and 100 ml of iodic acid solution were added to the other and both sides were stoppered. Small crystals could be detected after 1 or 2 days at room temperature and harvesting was performed after 50 to 150 days by pushing out the gel and dispersing it in a small amount of water. This was followed by a second light wash, air-drying of the crystals on filter paper and finally by hand

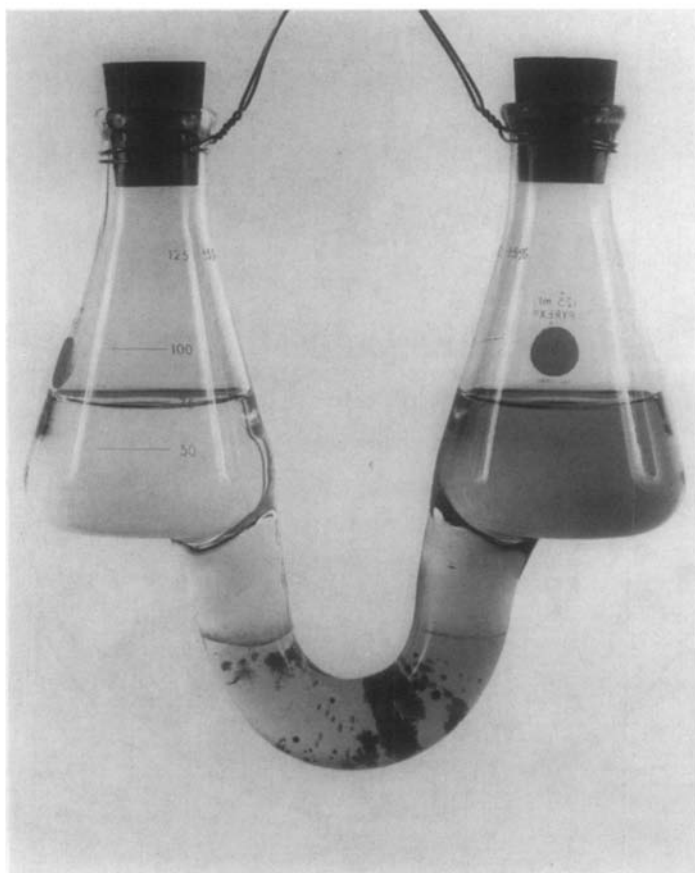


FIG. 2. Gel growth in large U-tube vessel.

picking. Growth runs were also sometimes performed using 1/2, 1/4, and 1/8 the copper sulfate and iodic acid solution strengths.

Some gels were set with sulfuric acid by using 12 ml concd  $H_2SO_4$  in 48 ml  $H_2O$  with 60 ml silicate solution added; all other conditions were identical. In one series of experiments copper was added to the gel: e.g., 1 ml of copper solution to 20 ml of gel, and after setting, 20 ml of iodic acid solution were added.

Characterization techniques used were the same as those described in I and II. Colors were designated by the names given in the supplement to NBS 533 (7).

### 3. Gel Growth at Room Temperature and Thermal Analysis Results

A photograph of a typical growth run after 50 days at room temperature using a gel set with acetic acid is shown in Fig. 3 together with a key identifying the five different types of crystals observed. Selected crystals of these phases are shown in Fig. 4.

Thermogravimetric analysis (TGA) showed two of these compounds to lose water, the  $Cu(IO_3)_2 \cdot \frac{2}{3}H_2O$  being the bellingrite previously described (confirmed by X-ray diffraction) and the other corresponding to  $Cu(IO_3)_2 \cdot 2H_2O$ , a

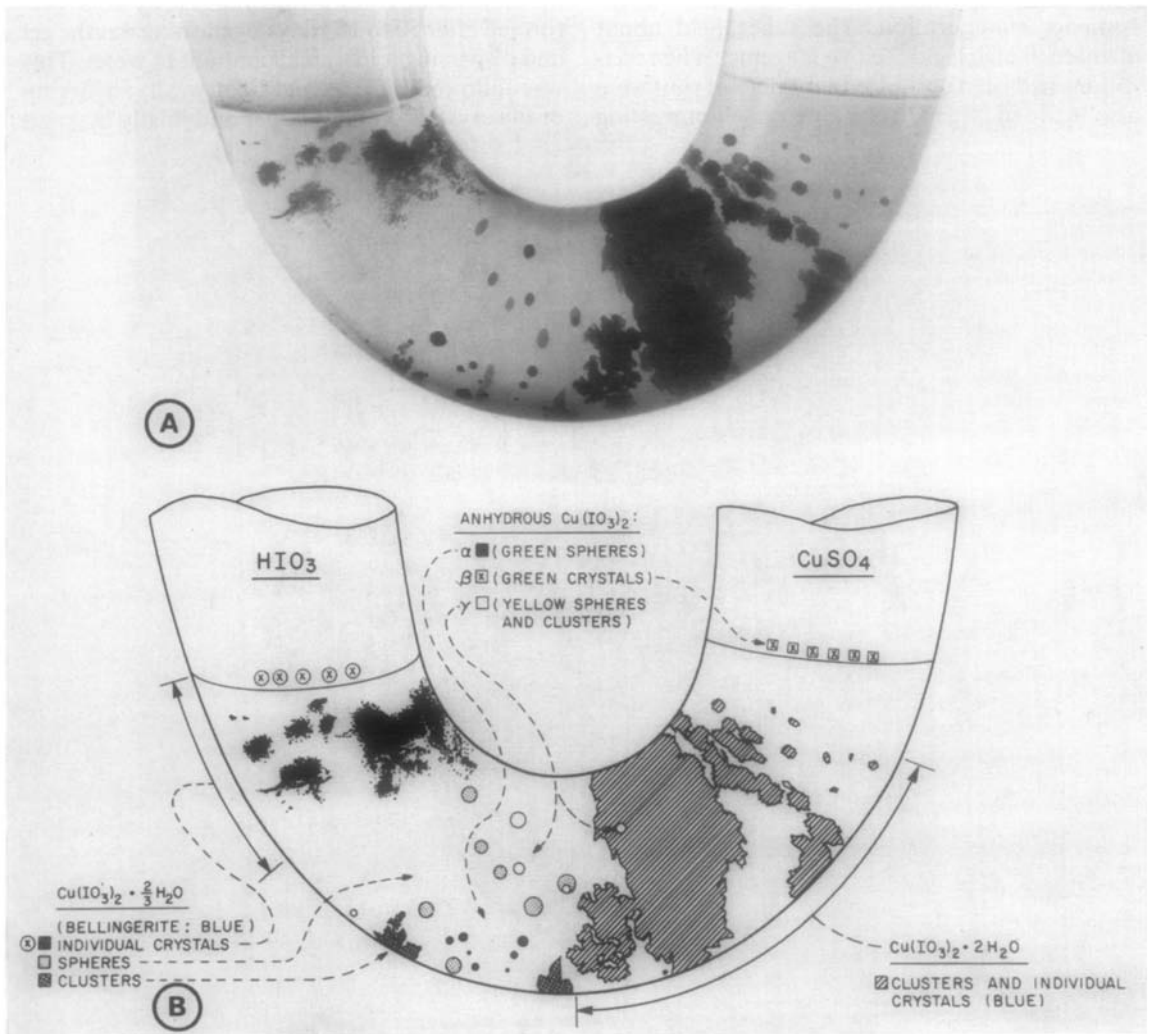


FIG. 3. Acetic acid set gel growth of copper iodates: (A) close-up of Fig. 2; (B) key.

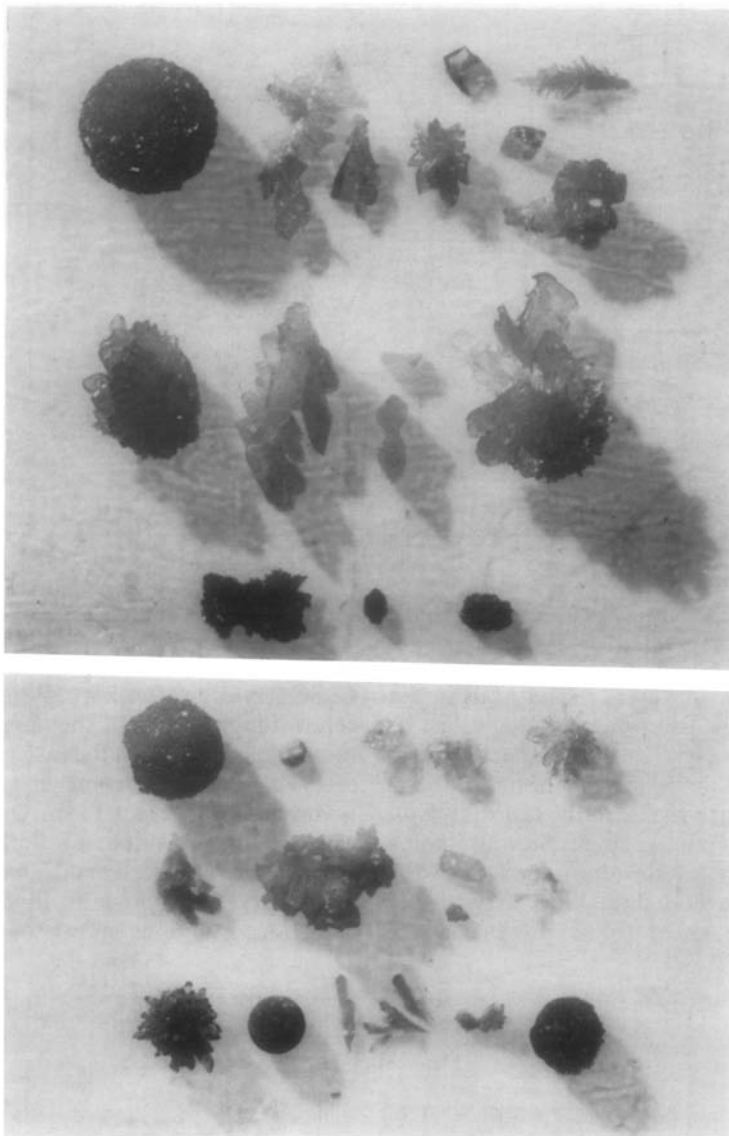


FIG. 4. Top to bottom: Crystals of  $\text{Cu}(\text{IO}_3)_2 \cdot \frac{1}{3}\text{H}_2\text{O}$  (bellingerite);  $\text{Cu}(\text{IO}_3)_2 \cdot 2\text{H}_2\text{O}$ ;  $\text{Cu}(\text{OH})\text{IO}_3$  (salesite);  $\alpha\text{-Cu}(\text{IO}_3)_2$ ;  $\beta\text{-Cu}(\text{IO}_3)_2$ ;  $\gamma\text{-Cu}(\text{IO}_3)_2$ . Largest sphere is 4 mm in diameter.

previously unreported phase. Both of these are light greenish-blue crystals of recognizably differing crystal morphologies (Fig. 4). Bellingerite grows as isolated crystals near and in the  $\text{HIO}_3$ , and as spherical agglomerates and clusters of crystals near the center of the gel. Dihydrate crystals, mostly in clusters, start near the center of the gel and extend toward the  $\text{CuSO}_4$  solution. No overlap was observed between the occurrence regions of the two hydrates.

The previously known anhydride, now designated  $\alpha\text{-Cu}(\text{IO}_3)_2$ , occurred in light yellowish-green spheres and spherical clusters in the central region as shown in Figs. 3 and 4. Also observed in this region was a new anhydride, designated  $\gamma\text{-Cu}(\text{IO}_3)_2$ , occurring as dark yellow spheres and spherical crystal clusters. A second new anhydride,  $\beta\text{-Cu}(\text{IO}_3)_2$  occurred as small deep bluish-green crystals which grew in the  $\text{CuSO}_4$  solution on the surface of the gel.

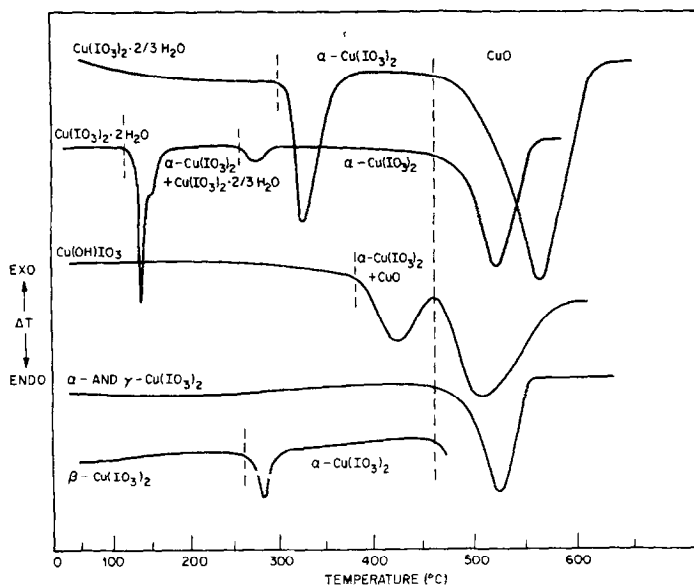


FIG. 5. Differential thermal analysis of copper iodates at 20°C/min under nitrogen.

The sequence of appearance of crystals in the acetic acid gel is the following: small clusters of bellingierite appear close to the iodic acid within 2 days; by the next day small spherulites of the  $\alpha$ - and  $\gamma$ -anhydrides are visible in the central region (some of these remain as spherulites and some transform into crystal clusters); crystals of the dihydrate form several days later. Crystals of  $\beta$ -anhydride were noted to be present in the

$\text{CuSO}_4$  solution after 2 wk. With the reagent concentrations at one half the above, the time-scale more than doubles. In the case of the sulfuric acid set gels growth is somewhat slower and the  $\alpha$ -anhydride does not form. Only bellingierite is observed in more dilute solutions in both systems.

The differential thermal analysis (DTA) and TGA curves are shown in Figs. 5 and 6 and all the transformations shown in these figures are

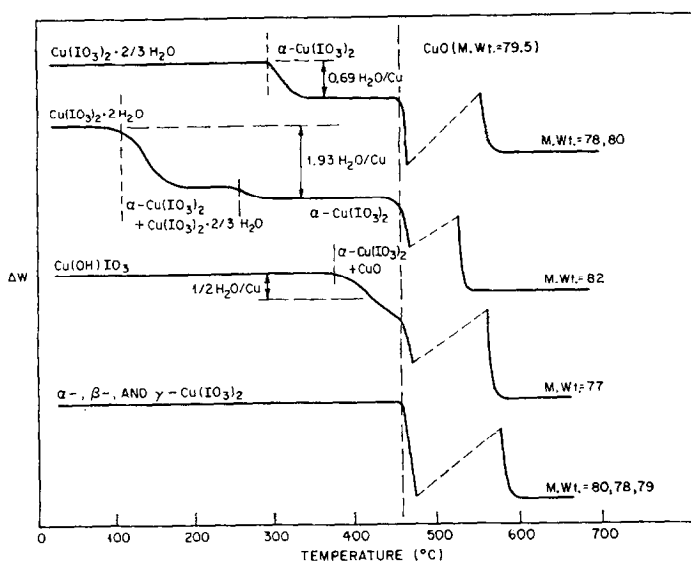


FIG. 6. Thermogravimetric analysis of copper iodates at 20°C/min under nitrogen.

TABLE I  
SUMMARY OF COPPER IODATES

Compound:	$\text{Cu}(\text{IO}_3)_2 \cdot \frac{3}{2}\text{H}_2\text{O}$ bellingerite	$\text{Cu}(\text{IO}_3)_2 \cdot 2\text{H}_2\text{O}^a$	$\alpha\text{-Cu}(\text{IO}_3)_2$	$\beta\text{-Cu}(\text{IO}_3)_2^d$	$\gamma\text{-Cu}(\text{IO}_3)_2^d$	$\text{Cu}(\text{OH})\text{IO}_3$ salesite
Color <sup>b</sup>	Light greenish blue	Light greenish blue	Light yellow green	Light green	Dark yellow	Deep bluish green
Decomposition temp (°C)	300	110	460	250	460	380
Form	Crystals, clusters, spherulites, dendrites	Crystals, clusters	Crystal clusters, spherulites	Crystal clusters, dendrites	Crystal clusters, spherulites	Crystals, clusters
Largest size crystals (mm)	2	5	1.5	1.5	1.5	1
Largest size spherulites (mm)	4	—	3	—	2	—
Refractive indexes (x, y, z)	1.90, 1.94, 1.96	1.89, 1.90, 1.94	1.88, 1.94, 2.00	1.90, 1.94, 1.96	1.89, 1.96, 1.99	1.78, 2.04, 2.05
Character and sign	Biaxial (+)	Biaxial (+)	Biaxial	Biaxial (-)	Biaxial (-)	Biaxial (-)
Optic angle (2V)	Small	Small	Medium	Large	Medium	Small
Point group <sup>c</sup>	I	2/m	2	I	2/m	mmm

<sup>a</sup> Probably thermodynamically metastable forms.

<sup>b</sup> Color designation according to supplement to NBS No. 553. (7).

<sup>c</sup> As determined by X-rays in IV (4).

represented schematically in Fig. 1. X-Ray powder diffraction patterns were employed to verify each step of Figs. 1, 5, and 6 for each compound. The decomposition temperatures are somewhat rate-dependent; they are reproducible within better than 10°C, but should not be considered more accurate than  $\pm 20^\circ\text{C}$ . The kinetics of the decomposition of bellingerite and  $\alpha$ -anhydride were studied by Lumme and Lumme (8), who determined reaction orders (1.6 and 0.7) and activation energies (107.9 and 77.7 kcal/mole). However, their results are based on the erroneous monohydrate formulation of bellingerite (3) and need to be corrected.

The transformation from  $\text{Cu}(\text{IO}_3)_2 \cdot 2\text{H}_2\text{O}$  to  $\text{Cu}(\text{IO}_3)_2 \cdot \frac{2}{3}\text{H}_2\text{O}$  was first observed during optical absorption measurements in a mineral oil mull as described in Sect. 7. Under these conditions essentially complete conversion occurred in less than 2 hr exposure in the light beams of either the Perkin-Elmer Model 421 or the Beckman IR-11 spectrophotometers. Heating of the powder in a thin layer (50°C for 72 hr or 100°C for 24 hr) however produced only  $\alpha$ -anhydride. That a specific photo-dehydration was not involved was proved by heating a mull in mineral oil overnight at 50°C, which produced essentially complete conversion to bellingerite; it appears the oil prevents the dissipation of the liberated water and so redirects the decomposition. Similarly storing finely ground dihydrate with a small amount of water at room temperature for 2 wk produces complete conversion to bellingerite; the same was subsequently also shown to be true of all three anhydrides.

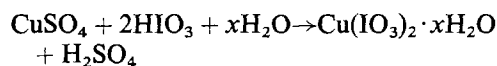
If any water evolved during heating of the dihydrate is not completely free to escape in the flowing gas stream, as during thermal analysis of a tightly packed sample, some bellingerite is produced as shown in Figs. 5 and 6; when heated in a single crystal form pseudomorphs after the dihydrate are formed, consisting of a mixture of bellingerite and the  $\alpha$ -anhydride.

All these phases are stable in the laboratory atmosphere over periods of months. However, as indicated in the summary of properties in Table I, it appears likely that the dihydrate and also the  $\beta$ - and  $\gamma$ -anhydrides are probably metastable phases in the thermodynamic sense at all temperatures. This tends to be a characteristic of products of the gel growth technique: e.g., in the case of  $\text{CaCO}_3$  the metastable phases aragonite and vaterite crystallize simultaneously with the stable calcite (5).

The compositions of bellingerite and the  $\alpha$ -anhydride were confirmed by analysis in I, and the TGA results of Fig. 6 combined with powder X-ray diffraction data of the decomposition products confirmed the composition of all the compounds discussed. In addition the molecular weight of the  $\text{CuO}$  remaining after TGA above 600°C was calculated, based on the formulations given, and values are given in Fig. 6. In all cases agreement of residue values and water content was well within the precision of the technique.

#### 4. Nucleation

In addition to the concentration gradients of both  $\text{CuSO}_4$  and  $\text{HIO}_3$ , the other major variable within the gel is the acidity. At the beginning of gel growth the acetic acid gel pH is about 5.5, while sulfuric acid gels and both reagents are in the 0.5 to 1.5 regions. Since the reaction,



where  $x = 0, 2/3, \text{ or } 2$ , liberates more acid, the later stages of growth in the acetic acid gels (pH then about 1), and all stages in the sulfuric acid gels occur in a fairly uniformly acidic medium with reagent concentration gradients expected to be the only significant factors. Reaction is not complete within the gel, in the sense that diffusion carries both reagents into each other with crystal growth of some bellingerite in the  $\text{HIO}_3$  solution and the  $\beta$ -anhydride in the  $\text{CuSO}_4$  solution in acetic acid gels at room temperature.

*A priori* one would have expected nucleation to be the major factor controlling the nature and location of the various phases growing in the gel. Accordingly a series of gel growth experiments were prepared in which a small amount of each of the five compounds, finely ground, was added to the initial gel mixture. Not enough material was available to ensure survival of actual seeds except in the bellingerite and  $\alpha$ -anhydride cases, but it was felt that a sufficient effect would remain from the probable survival of crystal embryos.

The  $\alpha$ -anhydride seeding experiment yielded the most dramatic effect, as shown in Fig. 7. Here particles of the  $\alpha$ -anhydride survived during gel setting, and enlarged somewhat for a few days. Several days later, however, crystals of the dihydrate began to grow in this region at the expense of the small  $\alpha$ -anhydride crystals, which were consumed in a spherical shell as shown in Fig. 7. One month later all traces of the  $\alpha$ -

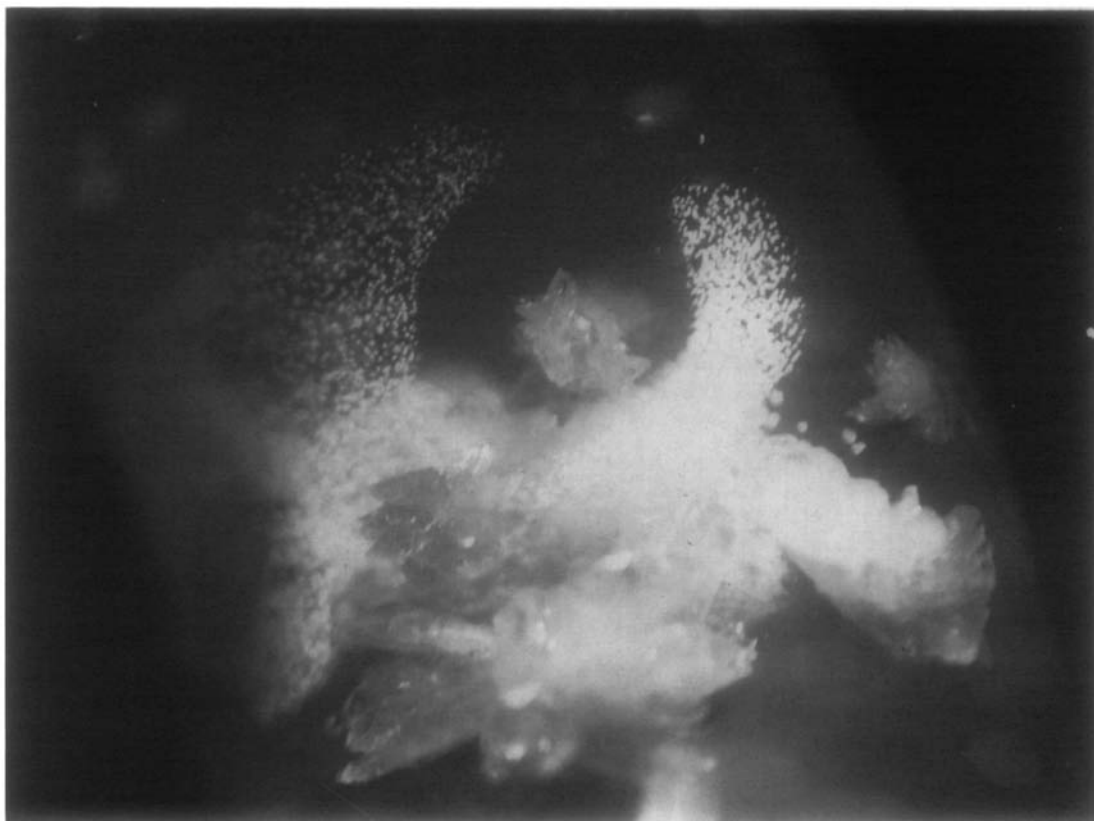


FIG. 7. Gel growth seeded with  $\alpha$ - $\text{Cu}(\text{IO}_3)_2$  showing dissolution and conversion to  $\text{Cu}(\text{IO}_3)_2 \cdot 2\text{H}_2\text{O}$ .

anhydride had disappeared, nor did any reform, even in regions where, in the absence of seeding, it usually crystallized. A possible explanation can be proposed based on a higher solution pressure of the many small crystals present in the seeded

gel: in the absence of seeding only a few large crystals of the  $\alpha$ -anhydride are present by the time the dihydrate forms; these are then stable with respect to the dihydrate.

Only the  $\gamma$ -anhydride seeded gel gave an

TABLE II  
RESULTS OF SEEDED GEL GROWTH EXPERIMENTS

Crystal sequence occurring in unseeded gel	$\text{Cu}(\text{IO}_3)_2 \cdot \frac{2}{3}\text{H}_2\text{O}$	$\alpha$ -Anhydride	$\gamma$ -Anhydride	$\text{Cu}(\text{IO}_3)_2 \cdot 2\text{H}_2\text{O}$	$\beta$ -Anhydride
Seeded with <sup>a</sup>					
$\text{Cu}(\text{IO}_3)_2 \cdot \frac{2}{3}\text{H}_2\text{O}$	+	-	-	-	-
$\text{Cu}(\text{IO}_3)_2 \cdot 2\text{H}_2\text{O}$	+	-	-	+	-
$\alpha$ - $\text{Cu}(\text{IO}_3)_2$	+	- <sup>b</sup>	-	+	-
$\beta$ - $\text{Cu}(\text{IO}_3)_2$	+	-	-	+	-
$\gamma$ - $\text{Cu}(\text{IO}_3)_2$	+	+	+	+	+

<sup>a</sup> + indicates present, - indicates absent.

<sup>b</sup> First present, then disappeared; see text.



essentially normal distribution of crystals as summarized in Table II. Seeding with bellingerite suppressed the formation of all other phases, but it was noted that some of the seed crystals which had fallen to the bottom of the gel in this case had no significant added growth on them, although in their immediate vicinity there grew a profusion of new crystals of much larger size. It is possible that this phenomenon is due to the absence of liquid

cusps (5) around the seed crystals; such cusps occur when the growing crystal pushes the gel aside and almost always form at self-nucleated crystals. In all cases the phases that did occur formed in essentially the same locations as in unseeded gel growth.

Most of these results can be explained on the basis that in the presence of water (if the pH is not too low) all phases convert to bellingerite, which



FIG. 8. Faceted dendrites of  $\text{Cu}(\text{IO}_3)_2 \cdot 3\text{H}_2\text{O}$  (field of view 1 cm).

then suppresses the nucleation of most other phases. The occurrence of the dihydrate in the three cases shown in Table II raises the possibility, not otherwise investigated, of this phase being an intermediate in some of these conversions to bellingerite. It must be noted that the gel growth of these iodates is not entirely reproducible. Despite careful cleaning, some seed-contamina-

tion apparently occurs at times and can result, for example, in the absence of any dihydrate.

### 5. Crystal Morphology

A surprisingly wide variation of crystal morphology is observed as can be seen in Fig. 4. In particular the crystal shapes ranged from isolated crystals (e.g., bellingerite) to faceted den-

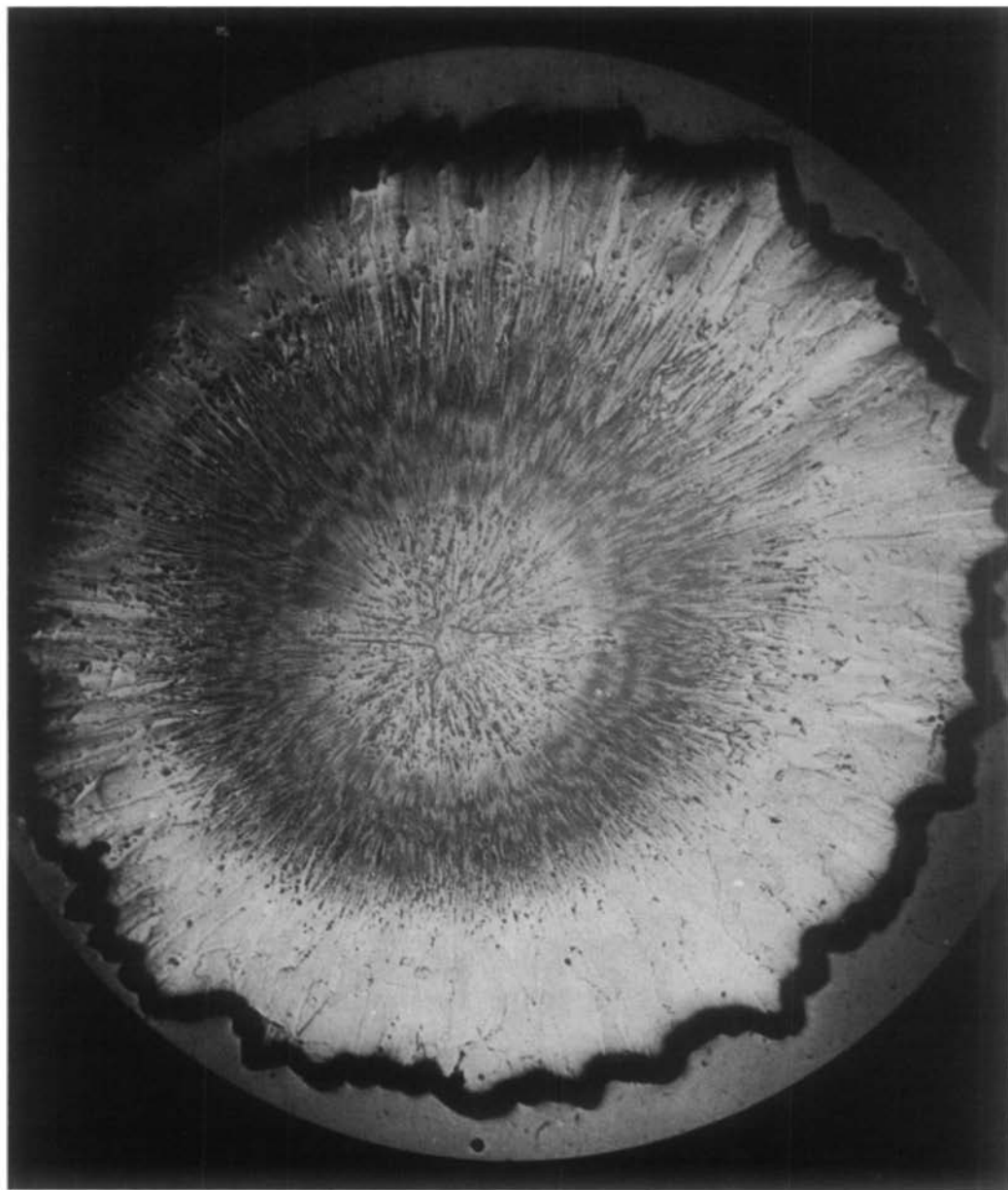


FIG. 9. Cross-section of globular spherulite of  $\text{Cu}(\text{IO}_3)_2 \cdot \frac{3}{2}\text{H}_2\text{O}$ ; diameter of sphere 3 mm.



FIG. 10. Coarse spherulite of  $\beta$ - $\text{Cu}(\text{IO}_3)_2$  growing on small sphere of  $\alpha$ - $\text{Cu}(\text{IO}_3)_2$  (overall diameter 4 mm).

drites (bellerite; also see Fig. 8) to wheat-sheave spherulites (dihydrate and  $\alpha$ -anhydride) to fine globular spherulites (bellerite,  $\alpha$ - and  $\gamma$ -anhydrides; also see Fig. 9) to overgrowth on spherulites both by coarse textured spherulites ( $\beta$ -anhydride; also see Fig. 10) and by crystals (bellerite,  $\alpha$ - and  $\gamma$ -anhydrides).

Some coarse textured dendrites were observed in acid gels with diluted reagents at room temperature. The crystals shown in Figs. 8 and 9, however, were obtained by mixing 0.1 to 5 cc of 0.6 *M* copper sulfate solution into 20 cc of acetic acid gel and, after setting, adding 20 cc of iodic acid solution. In the most concentrated case the dendrites of Fig. 8 formed in 6 days; in the weaker solutions globular spherulites of bellerite and  $\alpha$ -anhydride formed almost immediately, but these spherulites became covered with coarse

textured spherulites of the  $\beta$ -anhydride in 14 days as shown in Fig. 10.

Various forms of spherulites grown in "gelatine and jellies" have been described by Morse et al. (9, 10) for many different inorganic compounds, including manganese iodate (9). A recent treatment by Jackson (11) deals with the effect of diffusion, impurities, growth rate, and the entropy of crystallization on the full range of morphologies observed in melt growth. A treatment by Keith and Padden (12) discusses the non-equilibrium nature of spherulitic crystallization and notes the two apparently essential requirements of a fibrous habit and noncrystallographic small-angle branching. The rich phenomenology observed in the present work, with respect to both nucleation and morphology, clearly deserves detailed study.

## 6. Gel Growth at 60°C

Temperature has a significant effect on reactions in general, but a particularly large effect on both nucleation and diffusion. Accordingly gel growth experiments were also attempted in an oven at 60°C.

Growth was much more rapid than at room temperature and experiments were also conducted at 1/2, 1/4, and 1/8 the reagent concentrations. Bellingerite,  $\alpha$ -anhydride, and  $\beta$ -anhydride occurred in the acetic acid gels in that order, starting from the  $\text{HIO}_3$  end and close to it (apparently because the  $\text{Cu}^{2+}$  diffuses much more rapidly than the  $\text{IO}_3^-$  at the elevated temperature). In addition two extra phases appeared. In the  $\text{CuSO}_4$  solution a fine green powder formed rapidly at first, and was identified by X-ray powder diffraction as  $\text{Cu}_3(\text{OH})_4\text{SO}_4$ , also known by its mineral name antlerite; after some days, presumably as the acidity increased, the antlerite dissolved.

The second new phase occurred as deeply colored bluish-green crystals near the gel- $\text{CuSO}_4$  interface and were identified as the basic hydroxy iodate  $\text{Cu}(\text{OH})\text{IO}_3$ , also known as the mineral salesite (13). Details on this phase are also

included in Figs. 1 and 4, and in Table II; it decomposes on heating into a mixture of copper oxide and the  $\alpha$ -anhydride as shown by powder X-ray diffraction of a sample heated to 420°C. Salesite had been previously reported as prepared by precipitation (14), but we were unable to obtain it by following the given procedure (3), although others did report success (13, 15); possibly our laboratory was too contaminated with bellingerite seeds (analogous to our previous  $\alpha$ - $\text{Ni}(\text{IO}_3)_3 \cdot 4\text{H}_2\text{O}$  difficulties mentioned in I). Although originally thought to be dimorphs (13), the identity of mineral salesite and the synthetic product has been established (15).

At 60°C in the acetic acid gels the dihydrate did not form, and in the sulfuric acid gels neither the dihydrate nor the  $\gamma$ -anhydride formed. In the acetic acid gels bellingerite crystals were detectable within 1 day, and three anhydrides and salesite by 3 days; the sulfuric acid gels were not significantly slower. In the more dilute cases (e.g., 1/4 the reagent strengths) only bellingerite appeared to form in both types of gels. An additional pair of basic copper trihydroxy iodates, namely  $\text{Cu}_2(\text{OH})_3\text{IO}_3$  and  $\text{Cu}_2(\text{OH})_3\text{IO}_3 \cdot 2\text{H}_2\text{O}$ , have been reported (16-18); the only characterizations listed other than chemical analysis were

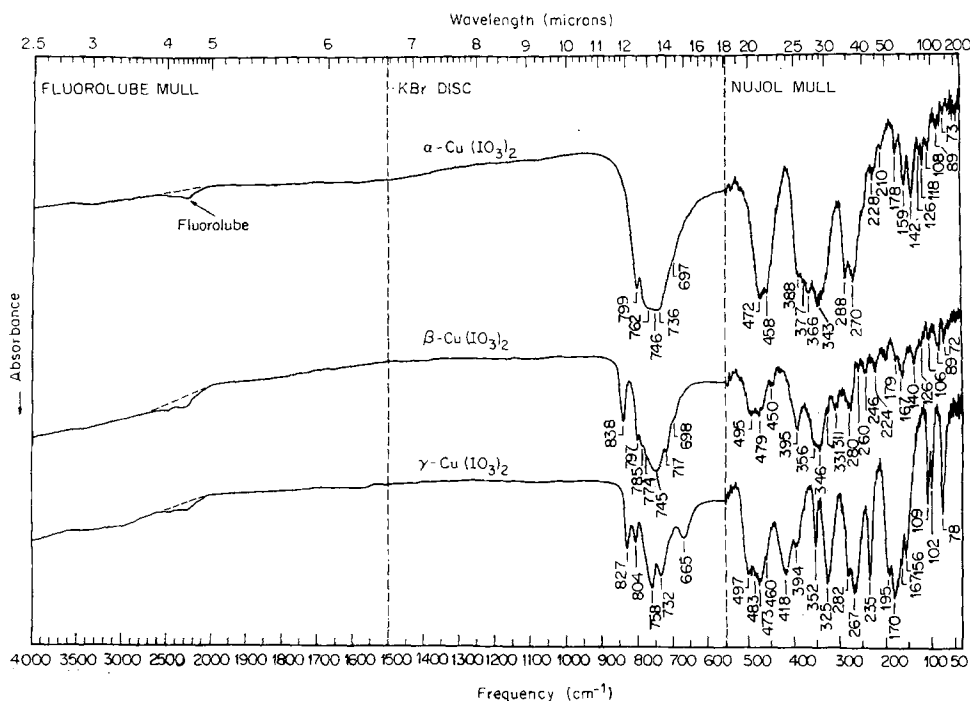


FIG. 11. Infrared absorbance curves of the anhydrous copper iodates.

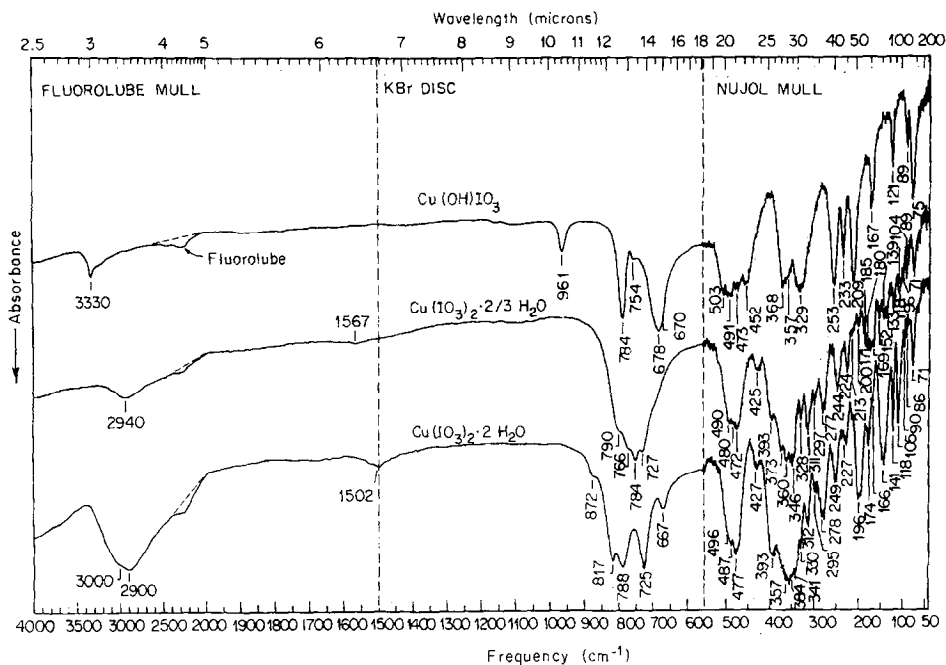


FIG. 12. Infrared absorbance curves of the hydrous copper iodates.

the TGA and infrared absorption bands (18). We did not attempt to reproduce these experiments.

## 7. Optical Data

Refractive indices and related optic data as determined on the petrological microscope are included in Table I. Optical absorbance data, determined as in I, are given in Figs. 11 and 12, and the diffuse reflectance data in Fig. 13.

The optical absorption data of Figs. 11 and 12 generally resemble the data given in I and the comments given there apply equally well here. The anhydrides show the absence, and the hydrous compounds the presence of OH. In the  $3000\text{ cm}^{-1}$  region strong hydrogen bonding is indicated for both hydrates; the hydroxy iodate salesite shows weak hydrogen bonding, the shift being only to  $3330\text{ cm}^{-1}$  from the unbonded value of about  $3600\text{ cm}^{-1}$ . The presence of a band in the  $1600\text{ cm}^{-1}$  region in both hydrates indicates water molecules; the absence of this band in salesite is consistent with the  $\text{Cu}(\text{OH})\text{IO}_3$  formulation.

In the prominent  $750\text{ cm}^{-1}$  region, containing bands originating from vibrations involving copper, iodine, and oxygen (see I), salesite stands

out. In this compound this region is different in shape from all the other iodates (and also from chlorates and bromates) reported in I as well as elsewhere (19), particularly in the well-separated  $961\text{ cm}^{-1}$  band.

All the iodates have six oxygens around each iodine, three at about  $1.8\text{ \AA}$  and three at  $2.5$  to  $3.0\text{ \AA}$ . In salesite one of the latter is an OH at  $2.50\text{ \AA}$  (15), and it is presumably the distortion in the coordination originating from the formally singly charged  $\text{OH}^-$  replacing a doubly charged  $\text{O}^{2-}$  that produces this unusual spectrum; the lower energy  $961\text{ cm}^{-1}$  band may then correspond to this weaker bond. The spectrum of the trihydroxy iodate  $\text{Cu}_2(\text{OH})_3\text{IO}_3 \cdot 2\text{H}_2\text{O}$  shows (18) similar characteristics in this region with bands at  $965\text{ (m)}$ ,  $895\text{ (m)}$ ,  $945\text{ (m,br)}$ ,  $775\text{ (s)}$ ,  $735\text{ (s)}$ , and  $700\text{ (w)}$   $\text{cm}^{-1}$ ; the first three bands were shifted by deuterium substitution, confirming the OH involvement.

The infrared spectra of the two hydrates are very similar, differing significantly only in the  $750\text{ cm}^{-1}$  and  $200\text{ cm}^{-1}$  regions. It was noted that on successive runs on the same sample of the dihydrate, either in KBr on the Perkin-Elmer Model 421, or in Nujol on the Beckman IR-11, a change toward the bellingerite pattern occurred.

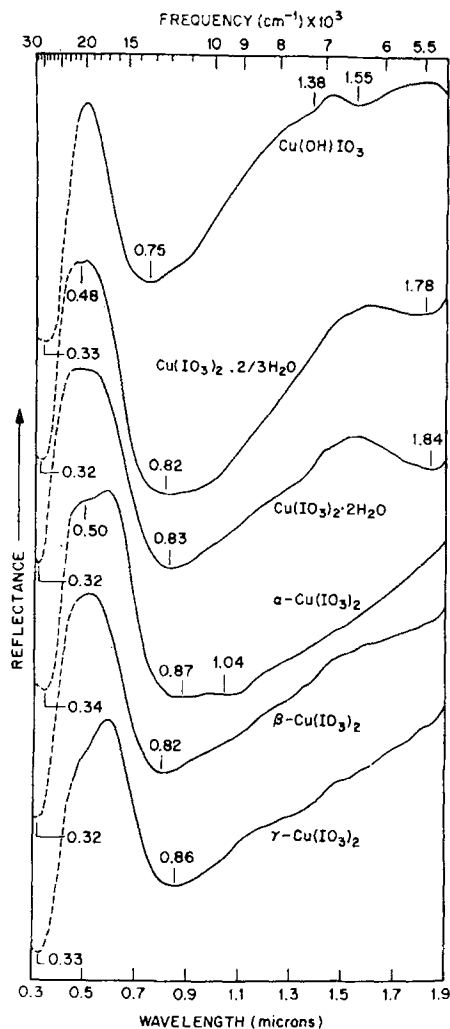


FIG. 13. Diffuse reflectance curves for the copper iodates in the ultraviolet, visible and near infrared.

As described in Sect. 3 above this change was observed by other techniques as well. The dihydrate absorption spectrum of Fig. 12 was taken rapidly using fresh samples for various regions of the spectrum so as to avoid any decomposition. In the case of the far infrared region of bellingerite, the use of a better sample gave a somewhat improved resolution over that in I. The results of diffuse reflectance measurements on fine powders are presented in Fig. 13. Here the visible region is dominated by the two copper absorptions near  $0.33 \mu\text{m}$  (charge transfer) and near  $0.8 \mu\text{m}$  (involving the  $E_g$  and

$T_{2g}$  levels), resulting in a green transmission band at  $0.5 \mu\text{m}$ ; in the case of the  $\gamma$ -anhydride this is shifted to about  $0.58 \mu\text{m}$ , giving the dark yellow color. Only the three hydrous compounds show OH combination and overtone bands in the 1 to  $2 \mu\text{m}$  region.

### Acknowledgments

We are grateful for extensive interactions with S. C. Abrahams, and to D. L. Wood and A. P. Ginsberg for helpful discussions.

### References

1. K. NASSAU, J. W. SHIEVER, AND B. E. PRESCOTT, *J. Solid State Chem.* **7**, 186 (1973).
2. S. C. ABRAHAMS, R. C. SHERWOOD, J. L. BERNSTEIN, AND K. NASSAU, *J. Solid State Chem.* **7**, 205 (1973).
3. K. NASSAU AND J. W. SHIEVER, *J. Inorg. Chem.*, **11**, 2552 (1972).
4. S. C. ABRAHAMS, R. C. SHERWOOD, J. L. BERNSTEIN, AND K. NASSAU, *J. Solid State Chem.* **8**, 274 (1973).
5. H. K. HENISCH, "Crystal Growth in Gels." Pennsylvania State Univ. Press, University Park, PA (1970).
6. J. W. SHIEVER AND K. NASSAU, *Mater. Res. Bull.* **7**, 613 (1972).
7. K. L. KELLY AND D. B. JUDD, *Nat. Bur. Stand. (U.S.) Circ. No 553* (including the supplement: Standard Sample No. 2106) U.S. Govt. Printing Office, Washington, DC (1965).
8. P. LUMME AND H. LUMME, *Suom. Kemistilehti B* **35**, 129 (1962).
9. H. W. MORSE, C. H. WARREN, AND J. D. H. DONNAY, *Amer. J. Sci.* **23**, 421 (1932).
10. H. W. MORSE AND J. D. H. DONNAY, *Amer. Mineral.* **21**, 391 (1936).
11. K. A. JACKSON in "Progress in Solid State Chemistry" (H. Reiss, Ed.), Vol. 4, p. 53. Macmillan, New York (1967).
12. H. D. KEITH AND F. J. PADDEN, *J. Appl. Phys.* **34**, 2409 (1963).
13. C. PALACHE AND O. W. JARRELL, *Am. Mineral.* **24**, 389 (1939).
14. A. GRANGER AND A. DE SCHULTEN, *Bull. Soc. Chim. Fr.* **31**, 1027 (1904); *Bull. Soc. Fr. Mineral.* **27**, 137 (1904).
15. S. GHOSE, *Acta Crystallogr.* **15**, 1105 (1962).
16. J. GAUTHIER, *C. R. Acad. Sci.* **248**, 3170 (1959).
17. P. LUMME AND H. LUMME, *Suom. Kemistilehti B* **35**, 120 (1962).
18. P. RAMAMURTHI AND E. A. SECCO, *Can. J. Chem.* **48**, 3510 (1970).
19. R. A. NYQUIST AND R. O. KAGEL, "Infrared Spectra of Inorganic Compounds." Academic Press, New York (1971).